

1 **Microfluidics based exploration for quorum quenching** 2 **genes in Antarctic microbiomes**

3
4
5 Joseph White^{1,#}, Jorge Díaz-Rullo^{2,3,#}, Verónica Morgante¹, José Eduardo González-Pastor¹,
6 Aurelio Hidalgo^{2,3,4*} and Mercedes Sánchez-Costa^{1,*}

7
8 ¹Department of Molecular Evolution. Centro de Astrobiología (CAB), CSIC-INTA. Carretera
9 de Ajalvir km 4, Torrejón de Ardoz (28850). Madrid, Spain.

10 ²Department of Molecular Biology. Universidad Autónoma de Madrid. Campus de
11 Cantoblanco, Madrid 28049, Spain.

12 ³Centro de Biología Molecular Severo Ochoa (UAM-CSIC) Nicolás Cabrera 1, Madrid 28049,
13 Spain.

14 ⁴Instituto de Biología Molecular. Universidad Autónoma de Madrid, Nicolás Cabrera 1,
15 Madrid 28049, Spain.

16 # indicates co-first authorship. Author order was determined by drawing straws.

17
18
19
20
21
22
23
24
25
26
27 * Corresponding authors: Mercedes Sánchez-Costa and Aurelio Hidalgo

28 Address correspondence to Mercedes Sánchez-Costa mersanchez@cab.inta-csic.es, or Aurelio
29 Hidalgo aurelio.hidalgo@uam.es

30 ABSTRACT

31 Quorum sensing (QS) is a form of microbial communication that enables each cell in a
32 population to sense the total population density, so that gene expression can be modified
33 accordingly. Quorum quenching (QQ) is the antagonistic disruption of this communication by
34 competing organisms, with potential use in the ongoing human effort to control microbial
35 populations. Previous studies have taken advantage of functional metagenomics to retrieve new
36 QS/QQ genes, but the frequency of obtaining positive clones remained very low, suggesting
37 the need for increased screening efficiency. Here, a new ultrahigh-throughput screening
38 method was developed to search for genes encoding novel QQ genes based on functional
39 metagenomics, microfluidics, and the development of an *Escherichia coli* reporter strain whose
40 fluorescence is repressed in the presence of AHLs but restored by the expression of any gene
41 that interferes with the QS system. This strain was transformed with a metagenomic short-
42 insert library collected from Antarctic plant rhizospheres; an understudied extreme
43 environment. The library was encapsulated in droplets containing single clones and sorted
44 using fluorescence-activated cell sorting (FACS). After screening approximately 7,000,000
45 clones, around 200 were recovered and one positive hit was confirmed, showing a previously
46 unreported mode of action that would have been difficult to detect using rational computational
47 methods. These findings underline the potential of microfluidics to dramatically increase
48 screening efficiency, while reducing costs and processing time, and they act as a proof of
49 concept for the discovery of more genes involved in QS and other molecular mechanisms of
50 interest in microbial ecology.

51 IMPORTANCE

52 Quorum sensing (QS) regulates essential microbial behaviours, including virulence, biofilm
53 formation, and symbiotic interactions, making it a key target for ecological and applied
54 microbiology. Disrupting QS through quorum quenching (QQ) has major potential in
55 agriculture, medicine, and biotechnology as an alternative to antibiotics or chemical treatments.
56 However, the discovery of QQ genes through brute-force approaches is limited by large
57 screening efforts, resulting in high costs and long processing times. Our study introduces a
58 microfluidics-based, ultrahigh-throughput functional screening platform that strongly
59 improves screening efficiency. It allowed us to identify a novel QQ gene, predicted to be
60 involved in a previously undescribed mechanism of QS disruption, from an under-explored
61 extreme environment (Antarctic rhizosphere). These results demonstrate how microfluidics can
62 optimise screening technologies, while unlocking the hidden functional diversity of microbial
63 communities useful for biotechnological applications in microbial control.

64

65

66

67

68

69 INTRODUCTION

70 Quorum sensing (QS) is a means of communication between microbial cells, allowing for cell
71 density-dependent control of gene expression (1). In its most basic form, a chemical signal
72 molecule, referred to as an ‘autoinducer’, is synthesised by microbial cells and released into
73 the environment. The concentration of this autoinducer increases at roughly the same rate as
74 the population density until a concentration threshold is crossed, whereupon the autoinducer
75 activates a positive-feedback loop by binding to a transcriptional regulator which upregulates
76 the expression of the autoinducer gene. Meanwhile, the same activated transcriptional regulator
77 binds to other promoter regions to alter the phenotype of the community in response to its high
78 cell density (1–3). This density-dependent communication enables a microbial species to build
79 a cooperative response to, for example, improve defence or access to nutrients, or to
80 differentiate into alternate morphological forms (4, 5).

81 Various types of autoinducer molecules have been described, but by far the most common are
82 the acyl-homoserine lactones (AHLs), usually known as AI-1. They are particularly widespread
83 in the Gram-negative proteobacteria (6, 7), while also having been detected in distantly related
84 organisms, such as cyanobacteria and even archaea (8–10). A classic example of QS that uses
85 an AHL as its autoinducer is found in the bacterium *Vibrio fischeri*, which provides the
86 luminescence for some marine animals. When this microorganism is distributed at low density
87 in open water, their QS relay is inactive. However, once it inhabits the light-emitting organ of
88 an animal, it quickly replicates within the confined space to a density where their AHL
89 autoinducer reaches the threshold concentration required to activate their transcriptional
90 regulator (LuxR), which then dimerizes and binds to specific promoters that contain a so-called
91 ‘lux box’ to regulate their activity. In this way, LuxR regulates the expression of its own *luxR*
92 gene and the *lux* operon, which contains the *luxI* autoinducer gene required for AHL
93 biosynthesis, as well as the luciferase genes that provides bioluminescence. This positive
94 autoregulation gives the system hysteresis, so that bioluminescence remains activated until the
95 bacterial population density decreases again (1, 6, 11–17).

96 Important as it is in aiding the establishment and dispersal of microbial communities, QS has
97 prompted the evolution of quorum quenching (QQ) systems that are able to disrupt it (18),
98 allowing antagonist species to compete more effectively with the QS species in their
99 environment. Mechanisms of QQ include inhibiting signal production, inactivating or
100 degrading the signal, inhibiting the signal reception by competing with the signal molecule’s
101 receptor analogues or by blocking the signal transduction cascade (19, 20). Such abilities have
102 been observed in a huge variety of different organisms, from prokaryotes to fungi, animals and
103 plants (21–26). There are three common classes of QQ enzymes that modify or degrade AHL
104 autoinducers: lactonases, acylases, and oxidoreductases (27, 28). The diversity of such
105 enzymes that has already been discovered suggests that these systems have evolved
106 independently on several occasions, representing a clear example of convergent evolution (22,
107 29), further demonstrating the importance and widespread use of QQ systems in nature.

108 Considering that bacterial virulence is often triggered by QS systems, it is of little surprise that
109 much interest has been directed towards QQ research, which represents a potential new means
110 of defence against microbial threats, particularly in the light of increasing resistance against
111 antimicrobial chemotherapy (30–32). Most of the QQ genes characterized so far have been
112 discovered using traditional cultivation-based techniques. However, this is slow and laborious

113 work, while also being untenable for the vast majority of prokaryotes, which remain
114 unculturable (33). As such, more and more laboratories are turning to metagenomics to ‘mine’
115 environmental samples for genes of interest (34–36), but this brute-force approach also requires
116 large screening efforts, resulting in high costs and long processing times, which significantly
117 limit its chances of success. These are particularly relevant factors when the frequency of
118 obtaining positive hits is very low as reported in previous functional metagenomics studies
119 searching for QS genes (Torres et al., 2018). To address these challenges, microfluidics offers
120 a powerful alternative enabling the manipulation of fluids at the micrometer scale by using
121 picoliter-sized droplets as test-tube analogues. This approach offers several advantages: i)
122 reduced volume, leading to lower reagent consumption and costs; ii) increased throughput; iii)
123 signal concentration within a confined space, and iv) minimized plastic use (37–41). Therefore,
124 in this work, a fluorescent QQ reporter strain, developed using modified genetic components
125 taken from the *lux* operon of *V. fischeri*, was used in conjunction with cultivation-independent
126 functional metagenomics and high-throughput microfluidic screening coupled to fluorescence-
127 activated cell sorting (FACS) to search for novel QQ genes from microorganisms harvested
128 from Antarctic rhizospheres.

129

130 **EXPERIMENTAL PROCEDURES**

131 **Bacterial strains, enzymes, oligonucleotides, constructs, media and culture conditions**

132 *Escherichia coli* DH10B (Invitrogen) was routinely grown in Lysogeny broth (LB) medium at
133 37 °C, 30 °C or 26 °C, depending on the type of plasmid it contained and the experiment.
134 Cultures were incubated routinely at 200 rpm, or 50 rpm when incubated on a Fisherbrand 3D
135 Platform Rotator (Fisher Scientific) to provide the swirling motion necessary to maintain 3-
136 oxo-C10-HSL suspension. When required, media was supplemented with 10 µM of 3-oxo-
137 C10-HSL. If appropriate, media were supplemented with sterile-filtered solutions of antibiotics
138 tetracycline (TET) 10 µg ml⁻¹, when selecting for clones transformed with the λ-red plasmid;
139 chloramphenicol (CHL) 40 µg ml⁻¹, when selecting for clones successfully recombined with
140 the *cat_luxR_gfp* cassette; and ampicillin (AMP) 100 µg ml⁻¹ for *E. coli* strains transformed
141 with pBluescript II SK + (pSKII+). Restriction enzymes, polymerases and T4 DNA ligase were
142 from New England Biolabs (UK) or Roche (Germany). Other chemicals were from Sigma-
143 Aldrich (Germany) and were at least of reagent grade purity. Electroporation was carried out
144 using a Micropulser (Bio-Rad) according to the manufacturer’s instructions.

145 **Construction of DH10B Δ*rbsAR*::*cat_luxR_gfp* reporter strain for quorum quenching**

146 The quorum quenching reporter cassette *cat_luxR_gfp* was constructed in three parts
147 chemically synthesized by IDT (Coralville, IA, USA). First, the CHL resistance *cat* gene with
148 Shine-Dalgarno sequence (BioBrick BBa_J31005) was combined with an upstream promoter
149 sequence (BioBrick BBa_I14033) and downstream sequence T10 terminator taken from the
150 pSB1C3 plasmid, as found on the iGem parts registry (http://parts.igem.org/Main_Page), with
151 non-coding sequences maintained (except for the addition of a *Bam*HI restriction site
152 downstream of the promoter). Second, the *luxR* gene from *V. fischeri* (BioBrick BBa_C0062)
153 was fused with a promoter (BBa_J23119) reverse orientated to avoid read-through, with three
154 base changes at positions 54T>A, 174C>A and 627C>T to remove restriction sites *Hind*III,
155 *Xba*I and *Pst*I, and with an artificial Shine-Dalgarno sequence, designed using the Salislab

156 website (https://salislab.net/software/OperonCalculator_EvaluateAnnotatedOperon) (42). The
157 *luxR* terminator was the modified *thr* terminator (BBa_B1006). Third, the *gfp* gene was taken
158 from pET28b.sfGFP together with its Shine-Dalgarno sequence (43), and expressed under a
159 modified version of the truncated λ phage constitutive promoter used by Pinheiro and
160 collaborators (44). The ‘lux box’ sequence was inserted between the -10 and -35 regions of the
161 truncated λ phage promoter, so that LuxR functioned as an AHL-dependent repressor at this
162 promoter, rather than as a transcriptional inducer as in the AHL autoinducer system of *V.*
163 *fischeri* (Fig. 1) (45).

164 The three synthetic parts of the whole construct were assembled by restriction, digestion and
165 ligation. Subsequently, they were integrated into the *rbsAR*, *arsB* and *lacZ* loci of the *E. coli*
166 DH10B chromosome by linear DNA recombination using the λ -red system (46). To facilitate
167 the homologous recombination, 200 bp homology arms were introduced at 5’-end of the *cat*
168 cassette and at the 3’ end of the *gfp* cassette. Competent *E. coli* DH10B cells were first
169 transformed with the λ -red plasmid by electroporation and the transformation plates incubated
170 in the dark at 30 °C overnight. The next day, LB-TET was inoculated with single colonies from
171 the transformation and incubated at 30 °C in the dark, overnight. LB-TET supplemented with
172 0.35 % L-arabinose was then inoculated with the previous day's overnight cultures (1:1000
173 dilution) and incubated in the dark at 30 °C until the OD₆₀₀ reached 0.2. At this point, they were
174 grown at 37 °C to induce the recombinant proteins of the λ -red plasmid, while also inhibiting
175 plasmid replication, and incubated until the OD₆₀₀ reached 0.4. Competent λ -red DH10B *E.*
176 *coli* cells were transformed with 1-2 μ g of the linear DNA cassette. Directly after
177 transformation, the cells were re-suspended in 1 ml of S.O.C. medium (ThermoFisher
178 Scientific) supplemented with 0.3 – 0.4 % L-arabinose and incubated at 37 °C overnight. The
179 next day, these cultures were spread onto LB-CHL agar plates and incubated at 37 °C to select
180 for recombinant clones. Modified regions were sequence verified.

181 To test the functionality of the reporter strain, the quorum-quenching *hqiA* gene, encoding a
182 lactonase (47), was excised from the original pME6010 plasmid by digestion with *BglII* and
183 *HindIII*. The resulting fragment was ligated into the multicloning site of pSKII+, previously
184 digested with *HindIII* and *BamHI*. The resulting construction (pSKII+*-hqiA*) was
185 electroporated into the reporter strain previously described. A strain transformed with an empty
186 pSKII+ plasmid was used as the negative control. Both strains were grown in LB with and
187 without 3-oxo-C10-HSL at 26 °C for 48 hours. Cultures were diluted in phosphate buffered
188 saline (PBS) to an OD₆₀₀ of 1, and fluorescence measurements were performed using a Qubit™
189 3 Fluorometer (Invitrogen) (λ_{ex} 430 to 490 nm, λ_{em} 510 to 580 nm). All measurements were
190 performed in triplicate. Microscopy was carried out with a fluorescence microscope Leica
191 CTR6000 (Leica Microsystems) coupled with a digital camera Hamamatsu C11440
192 (Hamamatsu Photonics Deutschland GmbH) using an excitation at 500/24 nm and an emission
193 at 542/27 nm when capturing fluorescence images.

194 **Development of an ultrahigh-throughput screening assay**

195 The fabrication of polydimethylsiloxane (PDMS) chips was carried out as previously described
196 (48, 49). Sylgard 184 silicone elastomer and Sylgard 184 curing agent (Sylgard) were mixed
197 at a mass ratio of 10:1, degassed in a liophilizer, poured on a clean silanized master
198 photolithographic mask with the embossed design for a 2-inlet, 20 μ m flow-focussing device
199 (available at <https://openwetware.org/wiki/DropBase>), and degassed a second time. The

200 covered masters were cured at 60 – 70 °C for > 3 hours, PDMS slabs were carefully cut away
201 and holes were punched for the inlets/outlets with a 1 mm diameter retractable biopsy punch
202 (KAI Medical). Chips were washed by immersion in a bath of isopropanol with ultrasound for
203 15 min, then washed in a bath of water with ultrasound for 15 min, before a final clean with
204 nitrogen gas and Scotch tape. Chips and clean glass slides were then treated with oxygen
205 plasma (200 W, 150 ml/min) and joined. To make fluorophilic chips, channels were flooded
206 with a 1 % solution of trichloro(1H,1H,2H,2H-perfluorooctyl) silane in HFE7500 (3 M)
207 fluorinated oil and incubated overnight at 65 °C. To make hydrophilic chips, channels were
208 flooded with 2 mg/ml poly(diallyldimethylammonium chloride) in 0.5 M NaCl, incubated at
209 room temperature for 10 min, flooded with 150 mM NaCl, then with 2 mg/ml poly(sodium 4-
210 styrenesulfonate) and incubated at room temperature for a further 10 min. Finally, the chips
211 were flooded with ultrapure water and stored in moist paper in a sealed container at room
212 temperature. All solutions were filtered through a 0.22 µm filter before use.

213 Cultures were grown overnight in LB-AMP-3-oxo-C10-HSL at 26 °C with swirling agitation,
214 then re-suspended in quarter-strength LB-AMP-3-oxo-C10-HSL to an OD₆₀₀ of 0.02. Single-
215 cell encapsulation was achieved by injecting the diluted cell culture and a 0.45 µm filtered
216 solution of 1.5 % (w/w) Fluosurf (Emulseo, France) in HFE7500 containing 10 µM 3-oxo-
217 C10-HSL through a fluorophilic flow focussing chip at flow rates of 100 and 1000 µL·h⁻¹,
218 respectively. At this culture dilution, the encapsulation of one cell per droplet in ca. 9.5 % of
219 the droplets was achieved, according to the Poisson distribution. Droplets, each around 4.5 pL,
220 were collected in a low binding 1.5 ml tube, the emulsion was spun briefly and the excess oil
221 removed with a syringe. Droplets were visualized in Fast-Read 102 slides with counting
222 chambers (Biosigma s.r.l., Italy) using an Olympus BX50 microscope equipped with FITC
223 fluorescence filters and a Pike F-032B camera (Allied Vision Technologies) and a 25X
224 objective to confirm the droplet occupancy and integrity before being incubated at 26 °C
225 overnight, with gentle agitation. After 12 h of incubation, the droplets were again imaged to
226 confirm cell growth within the occupied droplets. Droplets were then re-encapsulated in 1 %
227 (v/v) PBS-Tween using a 20 µm, hydrophilic, flow-focussing chips with a PBS:emulsion flow-
228 rate of 100:10. All solutions and emulsions were driven through the chips using the Cetoni
229 Nemesys Base 120 module and the Nemesys S pumps (Cetoni GmbH) and SGE gastight
230 syringes of adequate volume connected to microbore polyethylene tubing (Smiths Medical).
231 The microfluidic equipment was integrated by an inverted microscope (Leica DMi8) connected
232 to a high-speed camera (Fastcam Mini UX 50, Photron) for real-time visualization of
233 encapsulation experiments.

234 Emulsions were analysed and sorted using a FACSVantage SE (Becton Dickinson) at
235 approximately 400 events per second. 44,100 and 50,595 events were analysed for the positive
236 and negative control emulsions, respectively. Forward-scatter height (FSC-H) versus
237 fluorescence plot was used to differentiate between fluorescent versus non-fluorescent
238 droplets.

239 **Construction and screening of a metagenomic library from Antarctic plant rhizospheres**

240 The fluorescent reporter strain DH10B $\Delta rbsAR::cat_luxR_gfp$ was transformed with a
241 metagenomic library constructed with environmental DNA obtained from the rhizospheres of
242 two Antarctic plants: *Colobanthus quitensis* (Antarctic pearlwort) and *Deschampsia Antarctica*
243 (Antarctic hair grass), the only two flowering plants native to Antarctica. This original

244 combined library contained around 1,000,000 clones with insert sizes ranging from 2 – 5 kb
245 (50). DH10B $\Delta rbsAR::cat_luxR_gfp$ was transformed with a pool of plasmids isolated from the
246 original library, then grown in LB-AMP-3-oxo-C10-HSL until the cell culture reached an
247 $OD_{600} = 10$. The amplified new library was kept with 10 % glycerol (v/v) at $-80\text{ }^{\circ}\text{C}$.

248 To screen the library, a 0.5 ml-aliquot of the library was thawed and used to inoculate 1 ml of
249 LB-AMP-3-oxo-C10-HSL. Cultures were grown overnight at $26\text{ }^{\circ}\text{C}$ with swirling agitation,
250 then re-suspended in quarter-strength LB-AMP-3-oxo-C10-HSL to an OD_{600} of 0.02 and
251 encapsulated, incubated and reemulsified as described above for the control populations.
252 Emulsions were sorted by FACS using the previously established gating. Positive hits
253 recovered from FACS were suspended in 1 ml PBS and spread directly onto LB-AMP agar
254 plates. After incubation, recombinant colonies were replicated onto fresh plates and used to
255 inoculate liquid LB-AMP supplemented with 3-oxo-C10-HSL. After 48 h incubation at $26\text{ }^{\circ}\text{C}$,
256 all cultures were tested for green fluorescence using a benchtop Qubit™ 3 Fluorometer
257 (Invitrogen). Clones testing positive under these conditions were re-streaked twice more, to
258 ensure pure clonal colonies before being grown in culture. Plasmids were isolated from these
259 cultures using a QIAprep Spin Miniprep Kit (QIAGEN, Hilden, Germany) before being used
260 to transform DH10B $\Delta rbsAR::cat_luxR_gfp$, to rule out false positives caused by spontaneous
261 chromosomal mutations. New transformants were re-streaked twice before being used to
262 inoculate LB with and without 3-oxo-C10-HSL, alongside the original recovered hits and the
263 positive and negative controls, and incubated at $26\text{ }^{\circ}\text{C}$ for 48 hours. Resultant colonies were
264 streaked twice to again ensure pure clonal colonies before final cultures were incubated and
265 tested for fluorescence as before.

266 **Characterization of hits**

267 The positive hit recovered from FACS and confirmed by fluorescence testing after re-
268 transformation was sequenced by primer walking, and putative ORFs were predicted using
269 ORF Finder (<https://www.ncbi.nlm.nih.gov/orffinder/>) available at the NCBI website. For
270 translation of the predicted ORFs, bacterial and archaeal codes were selected, allowing for the
271 presence of alternative start codons. Predicted ORFs longer than 75 bp were used as queries in
272 protein-protein BLAST searches against non-redundant protein sequences for functional
273 assignment. Two halves of the original insert harbouring the putative identified ORFs were
274 cloned out of the plasmid by PCR using the plasmids reported in Table S1, and inserted into
275 empty pSKII+ by standard digestion and ligation with *XbaI/BamHI* (pAnt1-*orf1*) and
276 *HindIII/BamHI* (pAnt1-*orf2/3*) and fresh competent stocks of DH10B $\Delta rbsAR::cat_luxR_gfp$
277 were transformed with each construction. Obtained recombinant strains were confirmed by
278 sequencing. Similarly, *ybbA* gene from *E. coli* was cloned in pSKII+ by PCR, digestion and
279 ligation (Table S1). Newly transformed strains were re-streaked twice before being used to
280 inoculate LB with and without 3-oxo-C10-HSL, alongside the original complete hit and the
281 positive and negative controls and incubated at $26\text{ }^{\circ}\text{C}$ for 48 hours. All cultures were then re-
282 tested for fluorescence as described above in order to confirm which clone was responsible for
283 the observed fluorescence of the hit. Additionally, proteins encoded by pAnt1-*orf2/3* were
284 submitted to AlphaFold2 for structure prediction and evaluation of the quality of the predicted
285 folding (51).

286 **Testing for esterase/ABC-transporter activity**

287 Cultures of DH10B $\Delta rbsAR::cat_luxR_gfp$ harboring empty pSKII+, pAnt1-*orf2/3* or pSKII+-
288 *hqiA* were grown overnight in quarter-strength LB at 37 °C 200 rpm before being adjusted to
289 OD₆₀₀ of 0.6. For preparing protein extracts, 1.5 ml of the OD₆₀₀-adjusted cultures was
290 centrifuged at 16,000 x g for 2 min and cell pellets were re-suspended in 300 µl of BugBuster®
291 reactive (Novagen) by pipetting and vortexing for 10 s. After incubation at room temperature
292 for 20 min, samples were centrifuged at 16,000 x g for 30 min at 4 °C, and supernatants
293 containing the crude extracts were transferred to a clean tube. Fluorescence of each extract was
294 measured in Qubit™ 3 Fluorometer (Invitrogen) for verifying that the same quantity of GFP
295 was extracted from each strain. 10 µl of each extract was mixed with 100 µl of 0.1 × PBS with
296 HSL at a final concentration of 1 mM. As a negative control, another reaction was performed
297 without adding any protein extract. Reactions were incubated at room temperature for 1 h. 18
298 µl of reaction product was added to 2 ml tubes containing 582 µl of an overnight culture of the
299 reporter strain DH10B $\Delta rbsAR::cat_luxR_gfp$ in quarter-strength LB and adjusted to an OD₆₀₀
300 of 0.002. Cultures were incubated at 30 °C at 50 rpm for 16 h. As a positive control, 600 µl of
301 the OD₆₀₀-adjusted culture of the reporter strain was incubated without adding any reaction
302 product. 600 µl of each overnight culture were centrifuged at 16,000 x g for 2 min and the cell
303 pellet re-suspended in 200 µl PBS. Fluorescence was measured in in Qubit™ 3 Fluorometer
304 (Invitrogen). Fluorescence values were corrected with the OD₆₀₀ values of the final cultures
305 and the fluorescence values of the protein extracts.

306 **Statistical analysis**

307 Statistical parameters, including value of n, mean and standard deviation (S.D.), are reported
308 in Figure legends. One-way ANOVA followed by Tukey post hoc analysis was used to
309 calculate statistical significance using GraphPad Prism version 9.00 (GraphPad Software, La
310 Jolla, CA, United States).

311

312 **RESULTS**

313 **Construction of a reporter strain for quorum signal inhibition**

314 A strain derived from *E. coli* DH10B that expressed a quorum-signal dependent fluorescence,
315 designated as DH10B $\Delta rbsAR::cat_luxR_gfp$, was designed and constructed to detect genes
316 conferring quorum signal inhibition. The ‘fluorescence switch’ included a CHL resistance
317 gene, a transcriptional regulator gene *luxR* under the control of a constitutive promoter, and a
318 *gfp* gene under the control of a promoter containing a ‘lux box’ in a way that LuxR functioned
319 as an AHL-dependent repressor at this promoter (45) (Fig. 1A) (see Methods). The rationale
320 behind this QQ reporter strain is that presence of AHL would activate LuxR, repressing GFP
321 expression, while if this quorum signal response is disabled by the activity of a QQ transgene,
322 fluorescence would be restored (Fig. 1B). The reporter construct was inserted at *rbsAR*, *arsB*
323 and *lacZ* loci of *E. coli* DH10B chromosome, since these genes were previously characterised
324 as well non-essential insertion loci (52). However, only the strain in which the reporter
325 construct was inserted at *rbsAR* operon showed a clear fluorescent signal.

326 **Functional validation of reporter strain**

327 To test the functionality of this reporter construct, DH10B $\Delta rbsAR::cat_luxR_gfp$ strain was
328 transformed with the gene *hqiA*, which encodes for a previously identified QQ lactonase and

329 could therefore work as the positive control (DH10B $\Delta rbsAR::cat_luxR_gfp/pSKII+-hqiA$).
330 This lactonase, HqiA, shows homology with enzymes belonging to the cysteine hydrolase
331 (CHase) group that have been shown to cleave ether, ester and amide bonds, and it has the
332 ability to degrade a broad range of unsubstituted, oxo- and hydroxyl-substituted AHLs (29).
333 The strain was also transformed with empty pSKII+ to obtain a negative control (DH10B
334 $\Delta rbsAR::cat_luxR_gfp/pSKII+$).

335 Because HqiA lactonase was previously reported to show significantly higher efficacy of
336 degradation with long-chain AHLs such as 3-oxo-C10-HSL, and due to short-chain AHLs are
337 more prone to temperature-dependent lactonolysis than long-chain AHLs, 3-oxo-C10-HSL was
338 chosen for these functional assays (47, 53), being 10 μ M 3-oxo-C10-HSL was the minimal
339 concentration needed to abolish the signal (Fig. S1). Negative control showed strong
340 fluorescence in standard LB media lacking AHL, but repressed fluorescence after growth in
341 the presence of 3-oxo-C10-HSL, while the positive control strain maintained the same high
342 level of fluorescence regardless of the 3-oxo-C10-HSL concentration of the medium (Fig. 2).

343 Considering the correct functionality of the reporter, we implemented this assay in water-oil-
344 water (w/o/w) droplets using microfluidics. For that purpose, and prior to cell encapsulation,
345 each control strain was suspended in LB diluted to 25 % (v/v). This step was necessary for
346 reducing the background fluorescence produced by LB components that interferes with the
347 signal picked up from a fluorescent-cell occupied droplet, while sufficient nutrients are still
348 provided for overnight growth of encapsulated cells. Cells were double-encapsulated in w/o/w
349 droplets to allow for cell sorting in the hydrophilic matrix of most commercially available
350 FACS sorters. For double-encapsulation, cultures were first passed through a microfluidic chip
351 to create aqueous droplets within a stable oil matrix, using a biocompatible oil phase that
352 facilitates the transfer of respiratory gases (Fig. 3A). Cell-containing droplets were passed
353 through a hydrophilic microfluidic chip, where each droplet was encapsulated again in an outer
354 aqueous layer, creating double emulsions with an oil shell between two aqueous phases (54–
355 57). Double-encapsulated cells were incubated at 26 °C overnight in the presence of 3-oxo-
356 C10-HSL, as growth of the single cells would amplify the assay fluorescence signal and
357 facilitate FACS sorting (Fig. 3B-C). This microfluidic approach enabled the determination of
358 gating criteria for sorting positive events (Fig. 3C).

359 **Screening of a metagenomic library from the rhizosphere of Antarctic plants to search** 360 **for genes inhibiting QS**

361 To identify genes involved in QQ, a functional metagenomics approach was performed using
362 microfluidics to screen a large library from an understudied extreme environment. For that, the
363 DH10B $\Delta rbsAR::cat_luxR_gfp$ reporter strain was used as the host of a previously obtained
364 metagenomic library built in *E. coli* DH10B strain with the metagenomic DNA isolated from
365 the rhizomes of the Antarctic vascular plants *C. quitensis* and *D. Antarctica* clones in pSKII+
366 plasmid (50). Single metagenomic clones were double-encapsulated in the presence of 3-oxo-
367 C10-HSL and approximately 7,000,000 events were analysed and sorted as described above.
368 Using gating parameters previously set using control strains, 400 positive hits were recovered
369 from FACS (Fig. 4A) and plated on LB-AMP supplemented with 3-oxo-C10-HSL. After
370 overnight incubation, we obtained 222 recombinant clones. QQ phenotype of these clones was
371 validated by culture in the presence of 3-oxo-C10-HSL to fluorescence analysis. One
372 recombinant clone, called pAnt1, was confirmed as positive (Fig. 4B), which corresponds to

373 0.5 % positive clones showing QQ phenotype among the 222 filtered recombinant clones.
374 Moreover, considering that the sorted library contained 1,000,000 clones with a mean insert
375 length between 2 and 5 kb, the frequency of positive clones obtained with this ultrahigh-
376 throughput approach was 3×10^{-4} clones per Mbp.

377 **Identification and characterization of the gene involved in QS inhibition**

378 The complete sequence of the environmental DNA fragment harboured by the pAnt1 plasmid
379 was obtained by primer walking. This fragment of 2 kb contained three putative ORFs likely
380 to contain the gene of interest (Fig. 5). The pAnt1-*orf1*, located at the 5'-end of the fragment,
381 encoded for a protein truncated at the C-terminal similar to a FtsX-like permease family protein
382 from *Rhodanobacteraceae bacterium* (78.1% identity). pAnt1-*orf2* and pAnt1-*orf3* occupied a
383 similar region on the insert, though in different orientations. The reverse-orientated pAnt1-*orf2*
384 encoded for a protein that matched with an ABC transporter ATP-binding protein, most similar
385 to that found in the Gram-negative proteobacterium *Dokdonella fugitiva* (86.4% identity) and
386 harbouring a conserved YbbA protein domain. Meanwhile, the C-terminal truncated protein
387 encoded by the forward-orientated pAnt1-*orf3* showed similarity to an acyl-CoA thioesterase
388 I precursor from *Leclercia adecarboxylata*, but only with a 32.7% identity.

389 To determine which predicted ORF was responsible for the QQ phenotype, the upstream part
390 of the plasmid containing ORF1 and encoding an FtsX-like permease family protein (pAnt1-
391 *orf1*), and the downstream part harbouring ORF2 and ORF3 encoding the predicted esterase
392 and the ABC transporter ATP-binding protein (pAnt1-*orf2/3*) was individually sub-cloned into
393 the reporter strain. Subsequent fluorescence analysis confirmed all quorum-disrupting activity
394 to be associated with the downstream predicted ORF region (pAnt1-*orf2/3*) (Fig. 5B). A
395 possible explanation for this phenomenon could be that the predicted esterase activity of the
396 protein encoded by pAnt1-*orf3* degrades 3-oxo-C10-HSL, in a similar way to lactonases. The
397 alternative hypothesis was that the ABC transporter ATP-binding protein encoded by pAnt1-
398 *orf2* may be part of an ABC transporter that could export 3-oxo-C10-HSL from the cell.

399 To address whether the positive phenotype exhibited by pAnt1-*orf2/3* was caused by a
400 lactonase-like activity that degraded 3-oxo-C10-HSL, protein extracts of the DH10B
401 $\Delta rbsAR::cat_{luxR_gfp}$ strain harboring empty pSKII+, pAnt1-*orf2/3* or pSKII+*-hqiA* were
402 obtained and incubated with 3-oxo-C10-HSL. The reaction products were then added to
403 cultures of the reporter strain and fluorescence was measured. As expected, an increase in
404 fluorescence values was observed when the reporter strain was incubated with the protein
405 extract obtained from the positive control pSKII+*-hqiA* strain expressing the HqiA lactonase
406 (Fig. 5C). However, no differences in fluorescence values were observed when the reporter
407 strain was incubated with the protein extract obtained from the strain harboring pAnt1-*orf2/3*
408 (Fig. 5C). Instead, it showed similar fluorescence activity to that incubated with the empty
409 pSKII+ (negative control) protein extract (Fig. 6C). This result suggests that the pAnt1-*orf2/3*
410 QQ phenotype is not related to an AHL-degrading process. In addition to that, the AlphaFold2-
411 predicted structure of the proteins encoded by pAnt1-*orf2/3* exhibited low confidence metrics
412 for the putative esterase, with a predicted local distance difference test (pLDDT) score below
413 50 and substantial regions of disordered conformation (Fig. S2A).

414 In contrast, folding simulations of the predicted ABC transporter ATP-binding protein showed
415 a high confidence (pLDDT > 90) (Fig. S2B). Additionally, the uncharacterized ABC
416 transporter ATP-binding protein YbbA protein from *E. coli* was the closest match to the

417 putative ABC transporter ATP-binding protein encoded by ORF2 out of the structurally
418 characterized proteins available in UniProt/Swiss-Prot (52% identity). As such, it seemed a
419 more likely candidate, so we over-expressed YbbA in the reporter strain. However, the QQ
420 phenotype was still absent (Fig. S3). These data suggest that pAnt1-*orf2* would encode for a
421 protein showing a new biological activity related to QS inhibition.

422

423 DISCUSSION

424 With the creation of a new QQ reporter strain and its application in a microfluidics-based high-
425 throughput screening of a metagenomic library, this work has detected a novel QQ gene from
426 a hitherto little-investigated environment (Antarctic rhizospheres) and in doing so also
427 provided proof-of-principle for the viability of this approach.

428 Transgenes responsible for creating the fluorescence switch of the reporter strain included a
429 transcriptional regulator gene *luxR*, under the control of a constitutive promoter, as well as a
430 super-folding green fluorescent protein (*gfp*) gene under the control of a promoter with a 'lux
431 box' – a highly conserved, LuxR-binding DNA sequence – situated between its -10 and -35
432 sites. Genetic elements were recombined onto the chromosome of the reporter strain, rather
433 than being expressed from a plasmid, to increase stability and give a more consistent GFP
434 signal without the added variability of plasmid copy number. For that purpose, insertional locus
435 of the reporter construct in *E. coli* genome was critical, since an efficient chromosomal
436 integration of large DNA fragments tends to be problematic. Furthermore, both the *luxR*
437 transcriptional regulator gene and the 'lux box' sequence from the *lux* operon of *V. fischeri*
438 were modified in this work, so that the *luxI* (autoinducer) gene was absent, the *luxR* gene was
439 constitutively expressed, and only the *gfp* transgene was under the control of a 'lux box'
440 promoter. Normally, LuxR protein behaves as a transcriptional activator, but in this instance
441 the 'lux box' was modified to repress rather than amplify transcription with LuxR binding (58),
442 which is a relatively simple alteration, since the position of the lux-box with respect to the
443 promoter is thought to help determine its strength and function as an activator or a repressor.
444 Although this logic response has been questioned (59), context is so crucial in promoter
445 function that it continues to elude predictive computation (60, 61), and the AHL-repressible
446 promoter designed by Eglund and Greenberg has since undergone further validation (62). The
447 expression-repressing lux-box sequence and position described by Eglund & Greenberg was
448 tested in this design and, upon showing strong LuxR-controlled repression of the *gfp* gene, was
449 selected to work with (45).

450 This new QQ reporter offers some advantages over previous tools used in metagenomic studies
451 for the identification of new QS/QQ genes, such as the fluorescent *E. coli* AHL reporter, that
452 emits fluorescent signal in the presence of AHLs (63), or the *Chromobacterium violaceum*
453 CV026 biosensor, bacteria that produce a violaceous compound when exposed to AHLs (47, 64,
454 65). Among them: i) our reporter strain is designed to express fluorescence only when any QQ
455 gene is present in the cell; ii) it is sensitive and at least semi-quantitative, with variations in QQ
456 activity leading to different levels of GFP expression, and iii) it would be sensitive to any gene
457 product that interferes with the QS system, rather than being calibrated to identify enzymes
458 that degrade particular forms of AHL (66).

459 Another crucial element that must be considered in these kinds of studies is the AHL chosen.
460 All AHLs are composed of a homoserine lactone ring connected via an amide bond to an acyl
461 fatty acid side chain. They tend to vary in their composition by the length of this side chain
462 (generally 4 - 18 C atoms), the presence of unsaturated bonds within it and the existence, or
463 not, of an oxo- or hydroxyl group at the 3' position (6, 67, 68). In all their forms, AHL
464 molecules undergo lactonolysis, that is, the opening of the lactone ring by addition of a water
465 molecule in aqueous solutions. However, this process is slowed by a reduction in temperature
466 and pH, while AHLs with longer acyl chains are also naturally more resistant (69–74). In
467 addition, it was reported that the positive control HqiA lactonase exhibited a higher esterase
468 activity with long-chain AHLs such as 3-oxo-C10-HSL compared to AHLs with shorter chains.
469 For these reasons, 3-oxo-C10-HSL was chosen in this work, allowing for 48 h of cultivation in
470 swirling motion without any loss of signal, while abolishing fluorescence signal at a
471 concentration inside the biological range observed in nature (75, 76).

472 Furthermore, the identification of novel QS genes using functional metagenomics has been
473 successfully addressed by several laboratories in the past (47, 63–65). Therefore, in this work,
474 we have combined our reporter strain with functional metagenomics for the discovery of
475 environmental QQ genes. A metagenomic library constructed from an understudied, extreme
476 environment (the rhizome systems of two vascular Antarctic plants: *C. quitensis* (Antarctic
477 pearlwort) and *D. Antarctica* (Antarctic hair grass), which are the only two flowering plants
478 native to Antarctica) was used for the search. Better understanding of cold-adapted quorum
479 systems could be valuable, particularly in medicine and industry (77). Moreover, the soil
480 around rhizospheres is rich in QS-active microbes and is a hotspot for Gram-negative bacteria
481 that produce AHLs. As a result, several soil bacterial genera have been found to produce
482 enzymes that degrade AHLs (78–81).

483 In this work, the fact that only one QQ gene was discovered might suggest that while the
484 experimental pipeline was functioning as expected, there was an apparent paucity of QQ genes
485 within this Antarctic environment. However, it should be taken into account that the expected
486 number of positive clones was very low, attending to data from previous screens for QQ genes
487 (Table 1). It was estimated that the frequency of positive clones obtained using metagenome
488 screening varied between 1×10^{-4} to 3×10^{-3} per Mbp (47, 63–65), which is very similar to the
489 frequency reported here of 3×10^{-4} per Mbp. This suggests that the low abundance of QQ genes
490 in the Antarctic soil rhizosphere is similar to that found in other non-extreme environments.

491 This work also took advantage of microfluidics to dramatically reduce time processing and
492 costs. FACS pre-enrichment, analyzing 1,000,000 library clones through 7,000,000 droplet
493 events, reduced manual validation to 222 candidates. This represents a 4,500-fold reduction in
494 labor while maintaining detection sensitivity (3×10^{-4} per Mbp) comparable to other previous
495 studies in which traditional metagenomics was used to find novel genes involved in QS (Table
496 1). These data highlight the utility of high-throughput screening based on droplet sorting for
497 saving time, cost and reagents that may not be commercially available (i.e., AHLs) and
498 reducing the environmental footprint of the work when compared with plastic-based assays.
499 Additionally, this technique can be performed using equipment available in multiple research
500 facilities, contributing to high-throughput screening democratization.

501 The single hit that was recovered from the library proved to be a further surprise. Our data
502 suggests that the protein responsible for the QQ phenotype exhibited by pAnt1 is not related to

503 lactonase AHL degradation, which differs from the novel QQ genes discovered in previous
504 metagenomic studies (47, 63–65). In fact, pAnt1 analysis revealed that an ABC transporter
505 ATP-binding protein might cause the reported QQ phenotype. To the best of the authors'
506 knowledge, no ABC-transporter has been previously shown to impart a QQ phenotype.
507 Although it was largely assumed that all AHLs were freely diffusible in bacterial cells, such as
508 in *V. fischeri* or *E. coli*, it is known that certain species, such as *Pseudomonas aeruginosa*, are
509 not permeable to certain AHLs. In this bacterial species, the *mexAB-oprM* efflux pump is
510 involved in the active efflux of both long-chain AHLs like 3-oxo-C10-HSL, and short-chain
511 AHLs like C4-HSL, and the inactivation of this pump leads to the intracellular accumulation
512 of these AHLs (82). Therefore, one explanation for these data is that the predicted ABC
513 transporter ATP-binding protein encoded by pAnt1 has been retrieved from some
514 environmental microorganism that uses active transport through ABC transporters to export
515 AHLs out of the cell. However, if the observed QQ phenotype was caused by AHL efflux, the
516 environmental ABC transporter ATP-binding protein should be able to interact with any *E. coli*
517 ABC transporter permease with AHL transport potential, and to our knowledge, no AHL active
518 transporter has been reported to date. Thus, deeper characterization of this ABC protein will
519 be required to understand whether it represents a new QQ system that works by AHL active
520 transport. The novelty of this putative QQ gene underlines the importance of using screening
521 approaches not based only on sequence analysis, such as functional metagenomics, to discover
522 new bacterial molecular mechanisms.

523 In conclusion, we have developed the first ultrahigh-throughput functional screening for the
524 discovery of new QQ genes based on: i) microfluidic droplet sorting; ii) development of a
525 fluorescent QQ reporter strain, iii) construction of a metagenomic library from Antarctic plants
526 rhizosphere. This work verifies the importance of microfluidics for strongly increasing
527 efficiency and reducing costs when performing functional screenings, and provides a novel
528 fluorescent reporter strain sensitive to any gene product that interferes with the QS system.
529 Furthermore, this naïve strategy allowed for the discovery of a novel QQ gene with a potentially
530 previously unreported mode of action that would have been difficult to detect using
531 computational methods. Libraries from other environments, large-insert libraries or different
532 reporter strains based on other molecular mechanisms will be used in future ultrahigh-
533 throughput screenings for expanding our knowledge of quorum systems.

534

535 **DATA AVAILABILITY STATEMENT**

536 The datasets presented in this study can be found in online repositories. Names of the
537 repository/repositories and accession number(s) can be found below:
538 <https://www.ncbi.nlm.nih.gov/nuccore/PP836139>

539 **AUTHOR CONTRIBUTIONS**

540 Experiment design and performance: J.W., J.D.R., V.M., A.H., J.E.G.P., M.S.C.; data analysis:
541 J.W., J.D.R., M.S.C.; manuscript writing and reviewing: J.W., J.D.R., V.M., A.H., J.E.G.P.,
542 M.S.C.

543 **FUNDING**

544 This work has received funding from the European Union’s Research and Innovation
545 Framework program Horizon Europe under Grant Agreement number 101081957
546 (“Bluetools“). The CBM is funded by “Centre of Excellence Severo Ochoa” Grant CEX2021-
547 001154-S from MCIN/AEI /10.13039/501100011033 and receives institutional support from
548 Fundación Ramón Areces. JDR was supported by an FPI fellowship from Universidad de
549 Alcalá (Spain) and by an FPU fellowship (FPU18/03583) from the Spanish Ministry of
550 Universities.

551 ACKNOWLEDGMENTS

552 We thank Inmaculada Llamas (Institute of Biotechnology, Biomedical Research Center
553 (CIBM), University of Granada, Granada, Spain) for the kind gift of *fpME6010::hqiA* plasmid.
554 We also thank Carolina González de Figueras from Centro de Astrobiología (INTA-CSIC).
555 Finally, we acknowledge the Metafluidics project (Grant Agreement no. 685474) within the
556 framework of the Horizon 2020 programme for its contribution to the conceptualization and
557 early development of this work.

558

559 REFERENCES

- 560 1. Fuqua WC, Winans SC, Greenberg EP. 1994. Quorum sensing in bacteria: the LuxR-
561 LuxI family of cell density-responsive transcriptional regulators. *J Bacteriol* 176:269–
562 275.
563
- 564 2. Williams P, Winzer K, Chan WC, Cámara M. 2007. Look who’s talking:
565 communication and quorum sensing in the bacterial world. *Philosophical Transactions*
566 *of the Royal Society B: Biological Sciences* 362:1119–1134.
567
- 568 3. Abisado RG, Benomar S, Klaus JR, Dandekar AA, Chandler JR. 2018. Bacterial
569 Quorum Sensing and Microbial Community Interactions. *mBio* 9.
570
- 571 4. Pappenfort K, Bassler BL. 2016. Quorum sensing signal-response systems in gram-
572 negative bacteria. *Nat Rev Microbiol* 14:576–588.
573
- 574 5. Vadakkan K, Choudhury AA, Gunasekaran R, Hemapriya J, Vijayanand S. 2018.
575 Quorum sensing intervened bacterial signaling: Pursuit of its cognizance and
576 repression. *Journal of Genetic Engineering and Biotechnology* 16:239–252.
577
- 578 6. Fuqua C, Greenberg EP. 2002. Listening in on bacteria: Acyl-homoserine lactone
579 signalling. *Nat Rev Mol Cell Biol* 3:685–695.
580
- 581 7. Abisado RG, Benomar S, Klaus JR, Dandekar AA, Chandler JR. 2018. Bacterial
582 quorum sensing and microbial community interactions. *mBio* 9:1–14.
583

- 584 8. Sharif DI, Gallon J, Smith CJ, Dudley E. 2008. Quorum sensing in Cyanobacteria: N-
585 octanoyl-homoserine lactone release and response, by the epilithic colonial
586 cyanobacterium *Gloeotheca* PCC6909. *ISME Journal* 2:1171–1182.
587
- 588 9. Zhang G, Zhang F, Ding G, Li J, Guo X, Zhu J, Zhou L, Cai S, Liu X, Luo Y, Zhang
589 G, Shi W, Dong X. 2012. Acyl homoserine lactone-based quorum sensing in a
590 methanogenic archaeon. *ISME Journal* 6:1336–1344.
591
- 592 10. Charlesworth J, Kimyon O, Manefield M, Beloe CJ, Burns BP. 2020. Archaea join the
593 conversation: detection of AHL-like activity across a range of archaeal isolates. *FEMS*
594 *Microbiol Lett* 367.
595
- 596 11. Nealson KH, Platt T, Hastings JW. 1970. Cellular control of the synthesis and activity
597 of the bacterial luminescent system. *J Bacteriol* 104:313–322.
598
- 599 12. Eberhard A. 1972. Inhibition and activation of bacterial luciferase synthesis. *J*
600 *Bacteriol* 109:1101–1105.
601
- 602 13. Showalter RE, Martin MO, Silverman MR. 1990. Cloning and nucleotide sequence of
603 *luxR*, a regulatory gene controlling bioluminescence in *Vibrio harveyi*. *J Bacteriol*
604 172:2946–2954.
605
- 606 14. Engebrecht J, Nealson K, Silverman M. 1983. Bacterial bioluminescence: Isolation
607 and genetic analysis of functions from *Vibrio fischeri*. *Cell* 32:773–781.
608
- 609 15. Devine JH, Shadel GS, Baldwin TO. 1989. Identification of the operator of the *lux*
610 regulon from the *Vibrio fischeri* strain ATCC7744. *Proc Natl Acad Sci U S A*
611 86:5688–5692.
612
- 613 16. Choi SH, Greenberg EP. 1992. Genetic dissection of DNA binding and luminescence
614 gene activation by the *Vibrio fischeri* LuxR protein. *J Bacteriol* 174:4064–4069.
615
- 616 17. Eberhard A, Burlingame AL, Eberhard C, Kenyon GL, Nealson KH, Oppenheimer NJ.
617 1981. Structural identification of autoinducer of *Photobacterium fischeri* luciferase.
618 *Biochemistry* 20:2444–2449.
619
- 620 18. Dong YH, Wang LH, Xu JL, Zhang HB, Zhang XF, Zhang LH. 2001. Quenching
621 quorum-sensing-dependent bacterial infection by an N-acyl homoserine lactonase.
622 *Nature* 411:813–817.
623
- 624 19. Grandclément C, Tannières M, Moréra S, Dessaux Y, Faure D. 2015. Quorum
625 quenching: Role in nature and applied developments. *FEMS Microbiol Rev* 40:86–
626 116.
627

- 628 20. Paluch E, Rewak-Soroczyńska J, Jędrusik I, Mazurkiewicz E, Jermakow K. 2020.
629 Prevention of biofilm formation by quorum quenching. *Appl Microbiol Biotechnol*
630 104:1871–1881.
631
- 632 21. Uroz S, D'Angelo-Picard C, Carlier A, Elasri M, Sicot C, Petit A, Oger P, Faure D,
633 Dessaux Y. 2003. Novel bacteria degrading N-acylhomoserine lactones and their use
634 as quenchers of quorum-sensing-regulated functions of plant-pathogenic bacteria.
635 *Microbiology (N Y)* 149:1981–1989.
636
- 637 22. Uroz S, Dessaux Y, Oger P. 2009. Quorum sensing and quorum quenching: The Yin
638 and Yang of bacterial communication. *ChemBioChem* 10:205–216.
639
- 640 23. Kalia VC, Purohit HJ. 2011. Quenching the quorum sensing system: Potential
641 antibacterial drug targets. *Crit Rev Microbiol* 37:121–140.
642
- 643 24. Uroz S, Heinonsalo J. 2008. Degradation of N-acyl homoserine lactone quorum
644 sensing signal molecules by forest root-associated fungi. *FEMS Microbiol Ecol*
645 65:271–278.
646
- 647 25. Dong Y, Zhang L. 2016. Quorum sensing and quorum-quenching enzymes. *J*
648 *Microbiol* 43:101–109.
649
- 650 26. Hartmann A, Schikora A. 2012. Quorum Sensing of Bacteria and Trans-Kingdom
651 Interactions of N-Acyl Homoserine Lactones with Eukaryotes. *J Chem Ecol* 38:704–
652 713.
653
- 654 27. Sikdar R, Elias M. 2020. Quorum quenching enzymes and their effects on virulence,
655 biofilm, and microbiomes: a review of recent advances. *Expert Rev Anti Infect Ther*
656 18:1221–1233.
657
- 658 28. Fetzner S. 2015. Quorum quenching enzymes. *J Biotechnol* 201:2–14.
659
- 660 29. Torres M, Uroz S, Salto R, Fauchery L, Quesada E, Llamas I. 2017. HqiA, a novel
661 quorum-quenching enzyme which expands the AHL lactonase family. *Sci Rep* 7:1–15.
662
- 663 30. Barczak AK, Hung DT. 2009. Productive steps toward an antimicrobial targeting
664 virulence. *Curr Opin Microbiol* 12:490–496.
665
- 666 31. Cegelski L, Marshall GR, Eldridge GR, Hultgren SJ. 2008. The biology and future
667 prospects of antivirulence therapies. *Nat Rev Microbiol* 6:17–27.
668
- 669 32. Machado I, Silva LR, Giaouris ED, Melo LF, Simões M. 2020. Quorum sensing in
670 food spoilage and natural-based strategies for its inhibition. *Food Research*
671 *International* 127.
672

- 673 33. Rappé MS, Giovannoni SJ. 2003. The uncultured microbial majority. *Annu Rev*
674 *Microbiol* 57:369–394.
675
- 676 34. Handelsman J. 2005. Metagenomics: Application of Genomics to Uncultured
677 Microorganisms. *Microbiology and Molecular Biology Reviews* 69:195–195.
678
- 679 35. Riesenfeld CS, Schloss PD, Handelsman J. 2004. Metagenomics: Genomic analysis of
680 microbial communities. *Annu Rev Genet* 38:525–552.
681
- 682 36. Rondon MR, August PR, Bettermann AD, Brady SF, Grossman TH, Liles MR,
683 Loiacono KA, Lynch BA, MacNeil IA, Minor C, Tiong CL, Gilman M, Osburne MS,
684 Clardy J, Handelsman J, Goodman RM. 2000. Cloning the soil metagenome: A
685 strategy for accessing the genetic and functional diversity of uncultured
686 microorganisms. *Appl Environ Microbiol* 66:2541–2547.
687
- 688 37. Neun S, Brear P, Campbell E, Tryfona T, El Omari K, Wagner A, Dupree P, Hyvönen
689 M, Hollfelder F. 2022. Functional metagenomic screening identifies an unexpected β -
690 glucuronidase. *Nat Chem Biol* 18:1096–1103.
691
- 692 38. Tauzin AS, Pereira MR, Van Vliet LD, Colin P-Y, Laville E, Esque J, Laguerre S,
693 Henrissat B, Terrapon N, Lombard V, Leclerc M, Doré J, Hollfelder F, Potocki-
694 Veronese G. 2020. Investigating host-microbiome interactions by droplet based
695 microfluidics. *Microbiome* 8:141.
696
- 697 39. Colin P-Y, Kintsès B, Gielen F, Miton CM, Fischer G, Mohamed MF, Hyvönen M,
698 Morgavi DP, Janssen DB, Hollfelder F. 2015. Ultrahigh-throughput discovery of
699 promiscuous enzymes by picodroplet functional metagenomics. *Nat Commun* 6:10008.
700
- 701 40. Cecchini DA, Sánchez-Costa M, Orrego AH, Fernández-Lucas J, Hidalgo A. 2022.
702 Ultrahigh-Throughput Screening of Metagenomic Libraries Using Droplet
703 Microfluidics, p. 19–32. *In* .
704
- 705 41. Blas-Muñoz L, Orrego AH, Hofmeister M, Martínez-Salvador J, Ortega C, Rondón
706 Berrio V, Díaz-Rullo J, Finnigan J, Charnock S, Fessner W-D, González-Pastor JE,
707 Hidalgo A. 2025. A Microfluidics-Based Ultrahigh-Throughput Screening Unveils
708 Diverse Ketoreductases Relevant to Pharmaceutical Synthesis. *Anal Chem* 97:20698–
709 20706.
710
- 711 42. Tian T, Salis HM. 2015. A predictive biophysical model of translational coupling to
712 coordinate and control protein expression in bacterial operons. *Nucleic Acids Res*
713 43:7137–7151.
714
- 715 43. Peeler JC, Mehl RA. 2012. Site-Specific Incorporation of Unnatural Amino Acids as
716 Probes for Protein Conformational Changes, p. 125–134. *In* .
717

- 718 44. Pinheiro LB, Gibbs MD, Vesey G, Smith JJ, Bergquist PL. 2008. Fluorescent
719 reference strains of bacteria by chromosomal integration of a modified green
720 fluorescent protein gene. *Appl Microbiol Biotechnol* 77:1287–1295.
721
- 722 45. Eglund KA, Greenberg EP. 2000. Conversion of the *Vibrio fischeri* Transcriptional
723 Activator, LuxR, to a Repressor. *J Bacteriol* 182:805–811.
724
- 725 46. Murphy KC. 1998. Use of bacteriophage λ recombination functions to promote gene
726 replacement in *Escherichia coli*. *J Bacteriol* 180:2063–2071.
727
- 728 47. Torres M, Uroz S, Salto R, Fauchery L, Quesada E, Llamas I. 2017. HqiA, a novel
729 quorum-quenching enzyme which expands the AHL lactonase family. *Sci Rep* 7:943.
730
- 731 48. Mazutis L, Gilbert J, Ung WL, Weitz DA, Griffiths AD, Heyman JA. 2013. Single-cell
732 analysis and sorting using droplet-based microfluidics. *Nat Protoc* 8:870–891.
733
- 734 49. Zinchenko A, Devenish SRA, Kintsjes B, Colin P-Y, Fischlechner M, Hollfelder F.
735 2014. One in a Million: Flow Cytometric Sorting of Single Cell-Lysate Assays in
736 Monodisperse Picolitre Double Emulsion Droplets for Directed Evolution. *Anal Chem*
737 86:2526–2533.
738
- 739 50. de Francisco Martínez P, Morgante V, González-Pastor JE. 2022. Isolation of novel
740 cold-tolerance genes from rhizosphere microorganisms of Antarctic plants by
741 functional metagenomics. *Front Microbiol* 13.
742
- 743 51. Jumper J, Evans R, Pritzel A, Green T, Figurnov M, Ronneberger O, Tunyasuvunakool
744 K, Bates R, Židek A, Potapenko A, Bridgland A, Meyer C, Kohl SAA, Ballard AJ,
745 Cowie A, Romera-Paredes B, Nikolov S, Jain R, Adler J, Back T, Petersen S, Reiman
746 D, Clancy E, Zielinski M, Steinegger M, Pacholska M, Berghammer T, Bodenstein S,
747 Silver D, Vinyals O, Senior AW, Kavukcuoglu K, Kohli P, Hassabis D. 2021. Highly
748 accurate protein structure prediction with AlphaFold. *Nature* 596:583–589.
749
- 750 52. Sabri S, Steen JA, Bongers M, Nielsen LK, Vickers CE. 2013. Knock-in/Knock-out
751 (KIKO) vectors for rapid integration of large DNA sequences, including whole
752 metabolic pathways, onto the *Escherichia coli* chromosome at well-characterised loci.
753 *Microb Cell Fact* 12:60.
754
- 755 53. Delalande L, Faure D, Raffoux A, Uroz S, D'Angelo-Picard C, Elasri M, Carlier A,
756 Berruyer R, Petit A, Williams P, Dessaux Y. 2005. N-hexanoyl-l-homoserine lactone,
757 a mediator of bacterial quorum-sensing regulation, exhibits plant-dependent stability
758 and may be inactivated by germinating *Lotus corniculatus* seedlings. *FEMS Microbiol*
759 *Ecol* 52:13–20.
760
- 761 54. Joanicot M, Ajdari A. 2005. Droplet control for microfluidics. *Science* (1979)
762 309:887–888.
763

- 764 55. Christopher GF, Anna SL. 2007. Microfluidic methods for generating continuous
765 droplet streams. *J Phys D Appl Phys*. IOP Publishing [https://doi.org/10.1088/0022-](https://doi.org/10.1088/0022-3727/40/19/R01)
766 [3727/40/19/R01](https://doi.org/10.1088/0022-3727/40/19/R01).
767
- 768 56. Gruner P, Riechers B, Chacòn Orellana LA, Brosseau Q, Maes F, Beneyton T, Pekin
769 D, Baret JC. 2015. Stabilisers for water-in-fluorinated-oil dispersions: Key properties
770 for microfluidic applications. *Curr Opin Colloid Interface Sci* 20:183–191.
771
- 772 57. Shang L, Cheng Y, Zhao Y. 2017. Emerging droplet microfluidics. *Chem Rev*
773 117:7964–8040.
774
- 775 58. Eglund KA, Greenberg EP. 2000. Conversion of the *Vibrio fischeri* transcriptional
776 activator, LuxR, to a repressor. *J Bacteriol* 182:805–811.
777
- 778 59. Cox RS, Surette MG, Elowitz MB. 2007. Programming gene expression with
779 combinatorial promoters. *Mol Syst Biol* 3:145.
780
- 781 60. Kincade JM, deHaseth PL. 1991. Bacteriophage lambda promoters pL and pR
782 sequence determinants of in vivo activity and of sensitivity to the DNA gyrase
783 inhibitor, coumermycin. *Gene* 97:7–12.
784
- 785 61. Pasotti L, Zucca S. 2014. Advances and computational tools towards predictable
786 design in biological engineering. *Comput Math Methods Med* 2014.
787
- 788 62. Zucca S, Pasotti L, Politi N, Casanova M, Mazzini G, Cusella De Angelis MG, Magni
789 P. 2015. Multi-faceted characterization of a novel luxR-repressible promoter library for
790 *Escherichia coli*. *PLoS One* 10:1–26.
791
- 792 63. Nasuno E, Kimura N, Fujita MJ, Nakatsu CH, Kamagata Y, Hanada S. 2012.
793 Phylogenetically Novel LuxI/LuxR-Type Quorum Sensing Systems Isolated Using a
794 Metagenomic Approach. *Appl Environ Microbiol* 78:8067–8074.
795
- 796 64. Riaz K, Elmerich C, Moreira D, Raffoux A, Dessaux Y, Faure D. 2008. A
797 metagenomic analysis of soil bacteria extends the diversity of quorum-quenching
798 lactonases. *Environ Microbiol* 10:560–570.
799
- 800 65. Tannières M, Beury-Cirou A, Vigouroux A, Mondy S, Pellissier F, Dessaux Y, Faure
801 D. 2013. A Metagenomic Study Highlights Phylogenetic Proximity of Quorum-
802 Quenching and Xenobiotic-Degrading Amidases of the AS-Family. *PLoS One*
803 8:e65473.
804
- 805 66. Last D, Krüger GHE, Dörr M, Bornscheuer UT. 2016. Fast, continuous, and high-
806 throughput (bio)chemical activity assay for N-acyl-L-homoserine lactone quorum-
807 quenching enzymes 82:4145–4154.
808

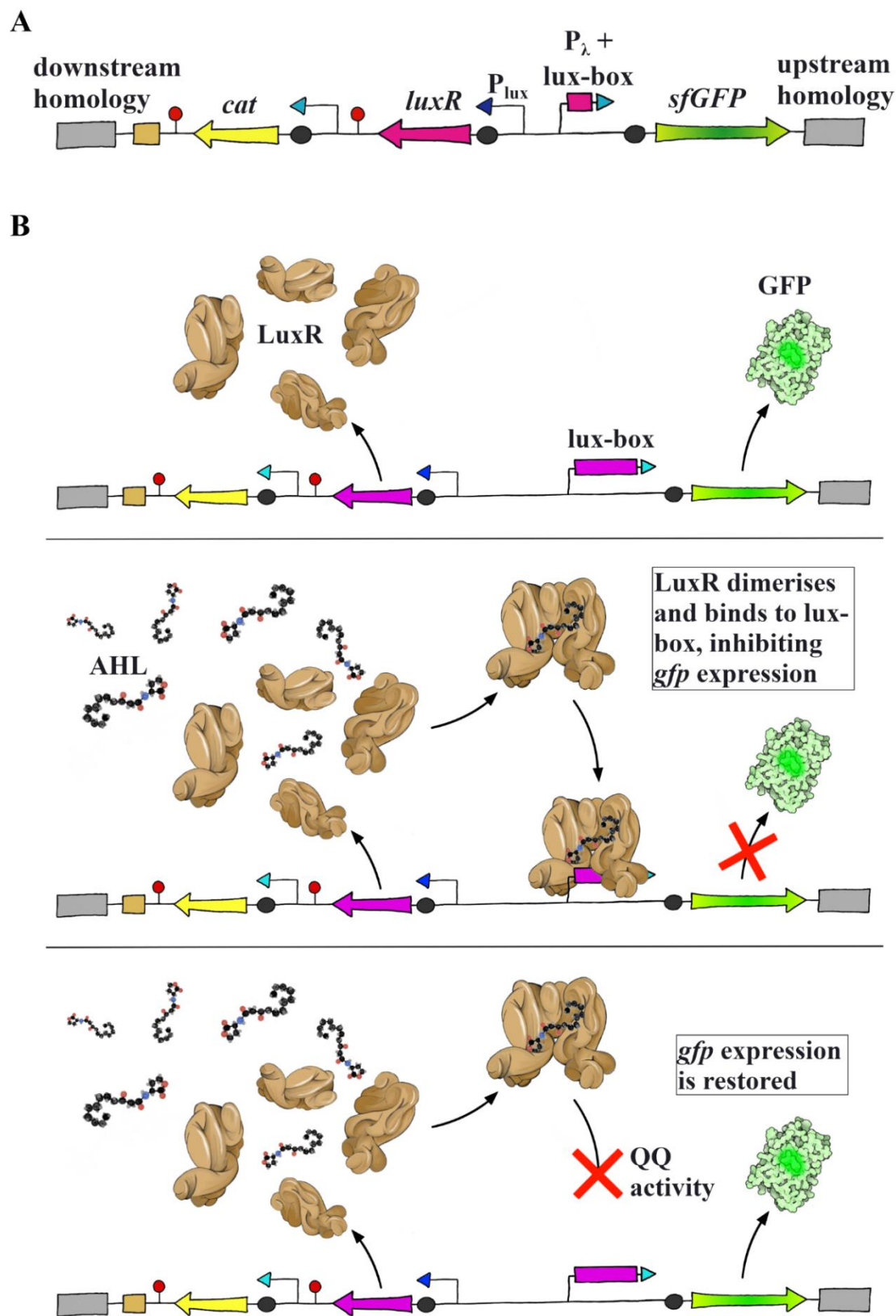
- 809 67. Galloway WRJD, Hodgkinson JT, Bowden SD, Welch M, Spring DR. 2011. Quorum
810 sensing in gram-negative bacteria: Small-molecule modulation of AHL and AI-2
811 quorum sensing pathways. *Chem Rev* 111:28–67.
812
- 813 68. Murugayah SA, Gerth ML. 2019. Engineering quorum quenching enzymes: Progress
814 and perspectives. *Biochem Soc Trans* 47:793–800.
815
- 816 69. Voelkert E, Grant DR. 1970. Determination of homoserine as the lactone. *Anal*
817 *Biochem* 34:131–137.
818
- 819 70. Decho AW, Visscher PT, Ferry J, Kawaguchi T, He L, Przekop KM, Norman RS,
820 Reid RP. 2009. Autoinducers extracted from microbial mats reveal a surprising
821 diversity of N-acylhomoserine lactones (AHLs) and abundance changes that may
822 relate to diel pH. *Environ Microbiol* 11:409–420.
823
- 824 71. Hmelo L, Van Mooy BAS. 2009. Kinetic constraints on acylated homoserine lactone-
825 based quorum sensing in marine environments. *Aquatic Microbial Ecology* 54:127–
826 133.
827
- 828 72. Miller C, Gilmore J. 2020. Detection of quorum-sensing molecules for pathogenic
829 molecules using cell-based and cell-free biosensors. *Antibiotics* 9:259.
830
- 831 73. Yates EA, Philipp B, Buckley C, Atkinson S, Chhabra SR, Sockett RE, Goldner M,
832 Dessaux Y, Cámara M, Smith H, Williams P. 2002. N-acylhomoserine lactones
833 undergo lactonolysis in a pH-, temperature-, and acyl chain length-dependent manner
834 during growth of *Yersinia pseudotuberculosis* and *Pseudomonas aeruginosa*. *Infect*
835 *Immun* 70:5635–5646.
836
- 837 74. Glucksam-Galnoy Y, Sananes R, Silberstein N, Krief P, Kravchenko V V., Meijler
838 MM, Zor T. 2013. The bacterial quorum-sensing signal molecule N-3-oxo-
839 dodecanoyl-L-homoserine lactone reciprocally modulates pro- and anti-inflammatory
840 cytokines in activated macrophages. *The Journal of Immunology* 191:337–344.
841
- 842 75. Kimbrough JH, Stabb E V. 2013. Substrate Specificity and Function of the Pheromone
843 Receptor AinR in *Vibrio fischeri* ES114. *J Bacteriol* 195:5223–5232.
844
- 845 76. Lupp C, Urbanowski M, Greenberg EP, Ruby EG. 2003. The *Vibrio fischeri* quorum-
846 sensing systems *ain* and *lux* sequentially induce luminescence gene expression and are
847 important for persistence in the squid host. *Mol Microbiol* 50:319–331.
848
- 849 77. Montgomery K, Charlesworth JC, LeBard R, Visscher PT, Burns BP. 2013. Quorum
850 sensing in extreme environments. *Life* 3:131–148.
851
- 852 78. Dong YH, Xu JL, Li XZ, Zhang LH. 2000. AiiA, an enzyme that inactivates the
853 acylhomoserine lactone quorum-sensing signal and attenuates the virulence of *Erwinia*
854 *carotovora*. *Proc Natl Acad Sci U S A* 97:3526–3531.

855
856
857
858
859
860
861
862
863
864
865
866
867
868
869
870
871

79. Flagan S, Ching WK, Leadbetter JR. 2003. *Arthrobacter* strain VAI-A utilizes acyl-homoserine lactone inactivation products and stimulates quorum signal biodegradation by *Variovorax paradoxus*. *Appl Environ Microbiol* 69:909–916.
80. Leadbetter JR, Greenberg EP. 2000. Metabolism of acyl-homoserine lactone quorum-sensing signals by *Variovorax paradoxus*. *J Bacteriol* 182:6921–6926.
81. Park SY, Lee SJ, Oh TK, Oh JW, Koo BT, Yum DY, Lee JK. 2003. AhlD, an N-acylhomoserine lactonase in *Arthrobacter* sp., and predicted homologues in other bacteria. *Microbiology (N Y)* 149:1541–1550.
82. Pearson JP, Van Delden C, Iglewski BH. 1999. Active Efflux and Diffusion Are Involved in Transport of *Pseudomonas aeruginosa* Cell-to-Cell Signals. *J Bacteriol* 181:1203–1210.

872

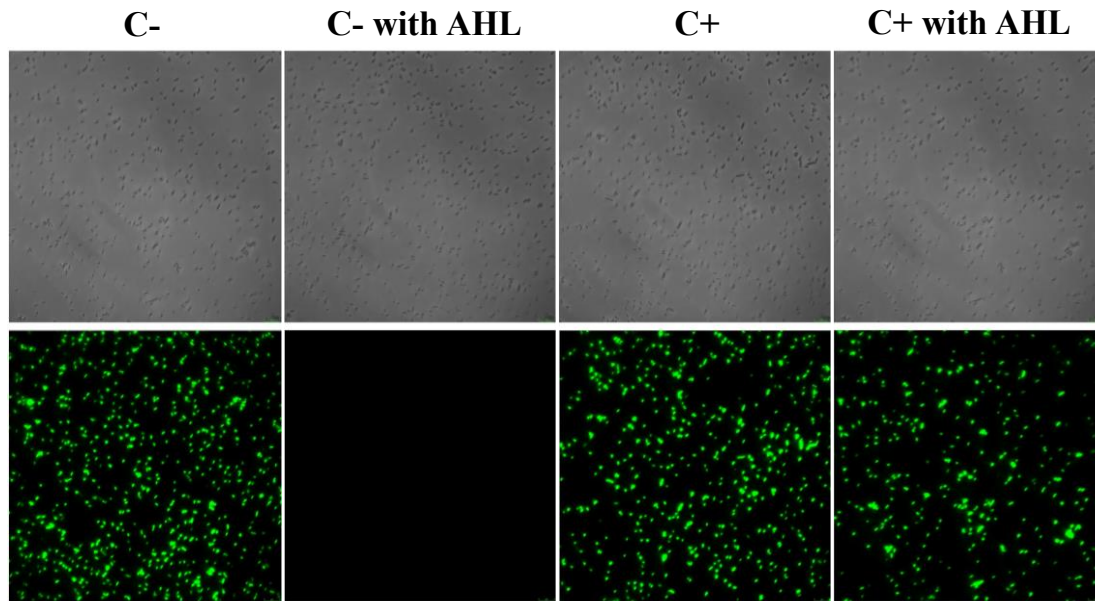
FIGURES



873

874 **Figure 1. Design and function of the *cat_luxR_gfp* reporter cassette (next page).**

875 **Figure 1. Design and function of the *cat_luxR_gfp* reporter cassette.** (A) Genetic construct
876 integrated at *rbsAR* locus. *cat*: chloramphenicol acetyltransferase gene; *luxR*: luxR family
877 transcriptional regulator gene; P λ +lux box: truncated constitutive P λ phage promoter with luxR
878 binding site, causing repression in the presence of luxR + homoserine lactone; sf-gfp: super-
879 folding green fluorescent protein gene; black circles: RBS sites; red lollipops: terminator
880 regions. (B) Top: The *luxR* gene produces LuxR protein under constitutive expression and GFP
881 under expression of the P λ phage promoter with lux-box. Center: The LuxR protein binds to the
882 AHL present in the medium. Once bound to AHL, the LuxR protein dimerizes and is able to
883 bind to the lux-box region of the truncated P λ phage promoter sequence, upstream of the *gfp*
884 gene. In doing so, it represses expression, and the GFP phenotype is abolished. Bottom: If a
885 QQ system is in play, the AHL will be made unavailable or the luxR will be prohibited from
886 binding to the DNA. Either way, *gfp* expression will remain active.
887
888

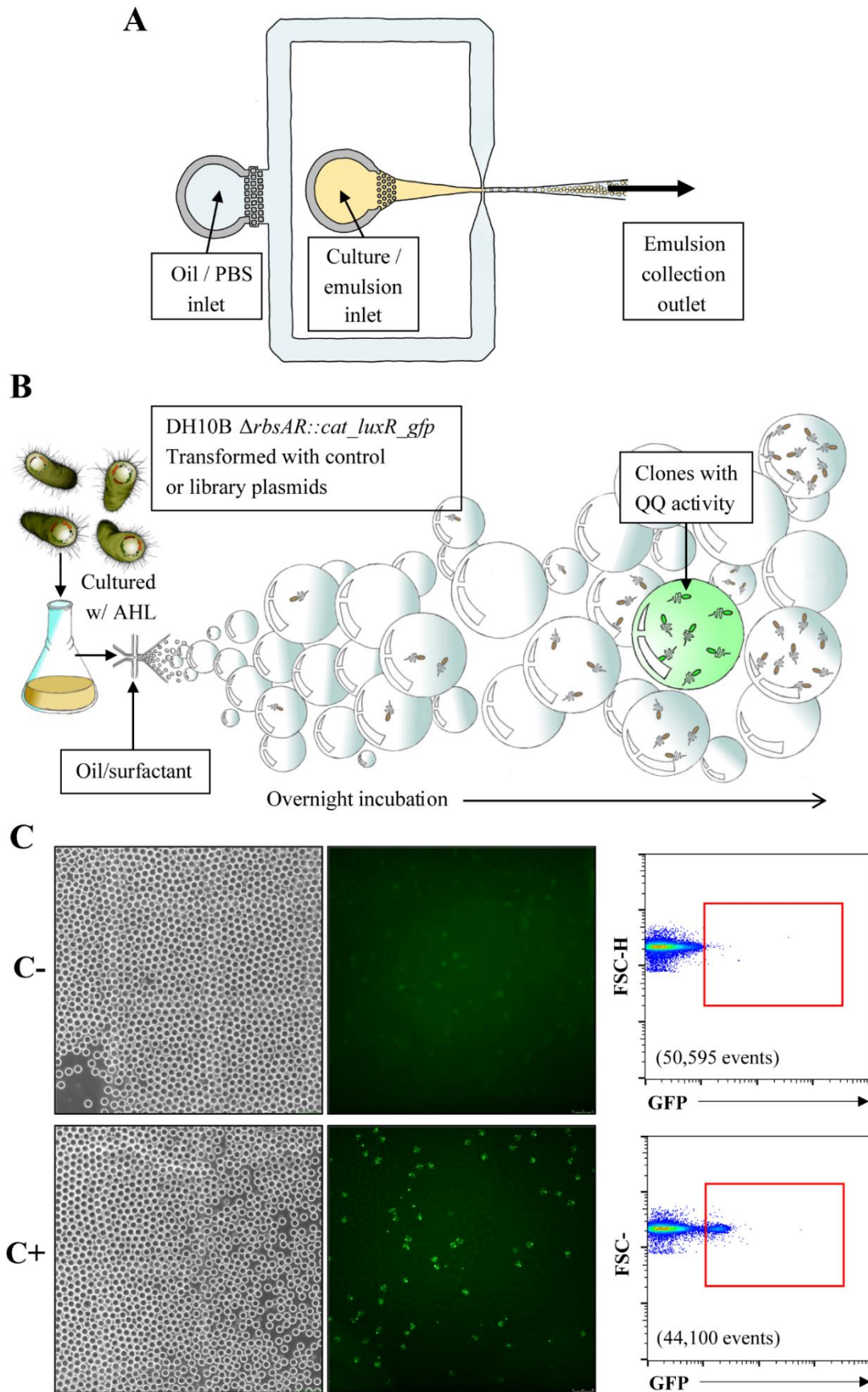


889
890

891 **Figure 2. HqiA lactonase gene successfully re-establishes fluorescence in the presence of**
892 **homoserine lactone.** DH10B $\Delta rbsAR::cat_luxR_gfp/pSKII+$ strain (negative control, C-) and
893 DH10B $\Delta rbsAR::cat_luxR_gfp/pSKII+-hqiA$ strain (positive control, C+) were grown with or
894 without 10 μ M 3-oxo-C10-HSL (AHL). All cultures grown at 26 °C for 48 h before re-
895 suspension in PBS to $OD_{600} = 1$. (top: phase contrast; bottom: green fluorescence;
896 magnification: 1000X).

897

898



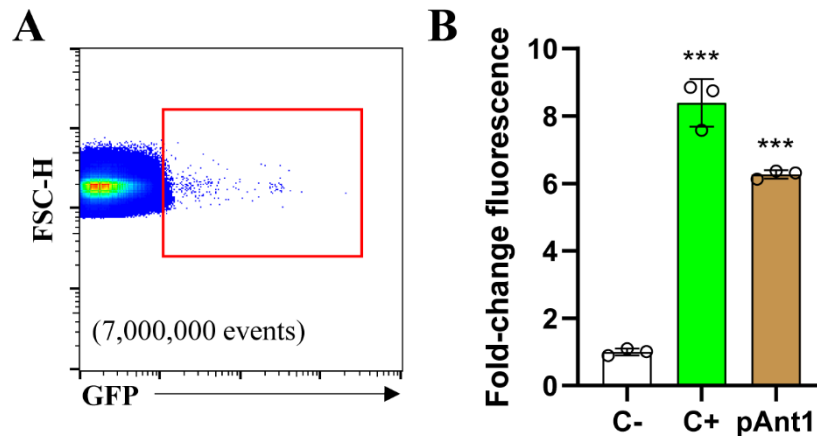
899

900 **Figure 3. Microfluidic approach for sorting cells showing QQ phenotype (next page).**

901 **Figure 3. Microfluidic approach for sorting cells showing QQ phenotype.** (A) Standard,
902 single-intersection chip with 20 μ M channel was used to encapsulate cells at a Poisson
903 distribution to ensure a maximum of 1 cell per droplet (giving 10 % occupation). (B) Droplets
904 harbouring DH10B $\Delta rbsAR::cat_luxR_gfp/pSKII+$ (negative control, C-) or
905 DH10B $\Delta rbsAR::cat_luxR_gfp/pSKII+-hqiA$ (positive control, C+) strains were incubated in
906 the presence of 10 μ M 3-oxo-C10-HSL at 26 °C overnight, allowing clonal cells to multiply
907 within their droplets. Those expressing QQ activity also expressed green fluorescence,
908 allowing detection by FACS. (C) Fluorescence microscope was used to take images of droplets
909 harbouring control strains (left: phase contrast; right: green fluorescence; magnification: 20X).
910 Droplets were sorted by FACS at approximately 400 events per second. 44,100 and 50,595
911 events were analysed for the positive and negative controls, respectively. Forward-scatter
912 height (FSC-H) versus fluorescence plot was used to differentiate between fluorescent versus
913 non-fluorescent droplets. Red boxes show population considered as positive.

914

915

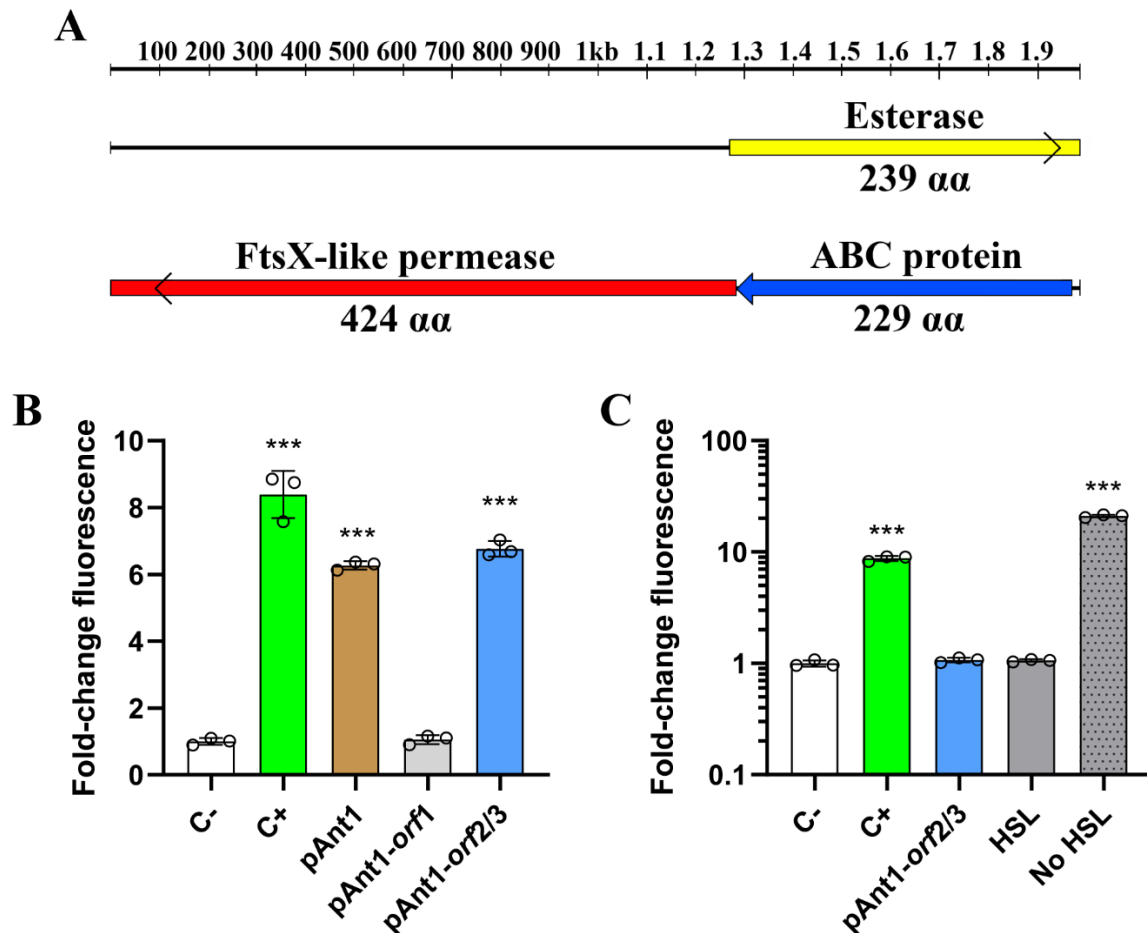


916

917 **Figure 4. Sorting of Antarctic library and identification of positive clone pAnt1.** (A)
918 DH10B $\Delta rbsAR::cat_luxR_gfp/pAnt_library$ was double-encapsulated in droplets and
919 incubated overnight at 26 °C in the presence of 10 μ M 3-oxo-C10-HSL. Droplets were sorted
920 by FACS at approximately 400 events per second, and approximately 7,000,000 events were
921 analysed. Red box inside FACS plot shows population recovered using the same gating criteria
922 fixed with the controls (Fig. 3). 400 positive hits were selected from FACS, and 222
923 recombinant clones were recovered. From these, one clone (pAnt1) showed a consistent
924 quorum inhibiting phenotype. (B). Fluorescence of pAnt1 or DH10B
925 $\Delta rbsAR::cat_luxR_gfp/pSKII+-hqiA$ (positive control, C+) in the presence of 10 μ M 3-oxo-
926 C10-HSL compared with DH10B $\Delta rbsAR::cat_luxR_gfp/pSKII+$ (negative control, C-; fold-
927 change). Strains were grown in 25 % LB supplemented with AMP and 3-oxo-C10-HSL for 48
928 h at 26 °C before resuspension in PBS to an OD_{600} of 1. One-way ANOVA followed by Tukey
929 post hoc analysis revealed the displayed significant differences against the negative control
930 (***) $p < 0.001$). Data represent the mean \pm S.D. (n = 3).

931

932



933
934

Figure 5. Characterization of pAnt1. (A) Schematic organization of the predicted ORFs identified in the fragment of eDNA harboured by the plasmid pAnt1. Arrows indicate the locations and the transcriptional orientation of the ORFs in the different plasmids. An open arrow near the corresponding end indicates truncated ORFs. (B) Fluorescence of DH10B $\Delta rbsAR::cat_luxR_gfp$ clones transformed with pSKII+ harboring *hqiA* lactonase gene (positive control, C+), pAnt1, pAnt1-orf1 or pAnt1-orf2/3 compared with reporter strain harboring empty pSKII+ (negative control, C-; fold-change). Strains were grown in 25 % LB supplemented with AMP and 10 μ M 3-oxo-C10-HSL for 48 h at 26 °C before resuspension in PBS to an OD₆₀₀ of 1. One-way ANOVA followed by Tukey post hoc analysis revealed the displayed significant differences against the negative control (**p < 0.001). Data represent the mean \pm S.D. (n = 3). (C) Fluorescence of the reporter strain DH10B $\Delta rbsAR::cat_luxR_gfp$ incubated with the products of the reactions of pure 3-oxo-C10-HSL with protein extracts obtained from DH10B $\Delta rbsAR::cat_luxR_gfp$ harboring empty pSKII+ (negative control, C-), pSKII+*-hqiA* (positive control, C+) or pAnt1-orf2/3. Fluorescence was normalized with the measurements of negative control (C-; fold-change). 10 μ L of protein extracts were mixed with 3-oxo-C10-HSL at a final concentration of 1 mM. After 1 h, reaction products were added to cultures of reporter strain, and cultures were incubated at 30 °C and 50 rpm for 16 h. Reporter strain was also incubated in the presence or absence of 10 μ M 3-oxo-C10-HSL (HSL and no HSL conditions, respectively). One-way ANOVA followed by Tukey post hoc analysis revealed the displayed significant differences against the negative control (**p < 0.001). Data represent the mean \pm S.D. (n = 3).

956 **Table 1. Metadata from previous studies reporting the discovery of new QS/QQ genes through non-ultrahigh throughput screening.**

Ref.	Environment	Reporter	Screened clones	Insert length	Positive clones	Positive clones per screened Mbp	Positive clones per screened clones
Nasuno 2012	Forest soil and an activated sludge from a coke plant in Japan	Fluorescent <i>E. coli</i> AHL reporter	103,700	40,000	3	7·E-04	3·E-05
Riaz 2008	Montrond soil samples (France)	<i>C. violaceum</i> CVO26 biosensor	10,121	40,000	1	3·E-03	9·E-05
Tannières 2013	Root microbiome of <i>S. tuberosum</i> plant treated with γ -caprolactone	<i>C. violaceum</i> CVO26 biosensor	29,760	40,000	1	8·E-04	3·E-05
Torres 2018	Hypersaline soil from Spanish saltern	<i>C. violaceum</i> CVO26 biosensor	250,000	40,000	1	1·E-04	4·E-06
This study	Antartic plant root rhizosphere	Fluorescent <i>E. coli</i> QQ reporter	1,000,000 (222 after FACS pre-enrichment)	3,500	1	3·E-04 (after FACS pre-enrichment)	5·E-03 (after FACS pre-enrichment)

957